

Insider information on successful covalent protein coupling with help from SpyBank

Anthony H. Keeble*, Mark Howarth*.¹

*Department of Biochemistry, University of Oxford, South Parks Road, Oxford, OX1 3QU, UK

¹Corresponding author: e-mail address: mark.howarth@bioch.ox.ac.uk

Contents

1. Introduction

2. SpyDesign – construction of successful SpyTag/SpyCatcher reagents

2.1 SpyBank database

2.2 Construct design

2.3 Cellular expression and purification

3. Analysis of SpyTag/SpyCatcher covalent coupling reactions

3.1 Reaction of components

3.2 Analysis of reaction

3.3 Conjugate purification

4. Concluding Remarks

Acknowledgements

References

Abstract

New biological properties can stem from the freedom to link, multimerize or multiplex protein building-blocks. The peptide SpyTag on one protein irreversibly reacts with SpyCatcher on another protein, through spontaneous isopeptide bond formation. Reaction is specific in a wide range of cellular environments and all components are genetically-encoded, making this chemistry accessible to molecular biologists. SpyTag/SpyCatcher has been widely used for enzyme immobilization, colocalization of different enzymatic activities, and increasing enzyme resilience. Here we present routes and advice for efficient design, expression and purification of SpyTag/SpyCatcher constructs in bacterial and eukaryotic environments, including the latest 002 variants, and how to analyze reaction efficiency. The SpyInfo webpage collates the different publications and patents using SpyTag/SpyCatcher, while the SpyBank database lists their sequences and expression routes. The ability of SpyTag/SpyCatcher to react in a broad range of situations creates diverse opportunities for augmenting the function of enzymes and other biomolecules.

Keywords: protein-protein interaction, synthetic biology, nanobiotechnology, nanoassembly, protein superglue, metabolite channeling, protein engineering, plug-and-display.

1. Introduction

Covalent coupling enables the construction of protein assemblies beyond nature or conventional genetic fusion. The SpyTag/SpyCatcher system has been termed a genetically-encoded click chemistry, without the complication of using any unnatural amino acids (Wang & Zhang, 2018). SpyCatcher fused to one protein irreversibly reacts with the SpyTag on another protein to form a spontaneous isopeptide bond (Figure 1A). The reaction is irreversible and specific in a range of cellular environments (Zakeri, Fierer, Celik, Chittock, Schwarz-Linek, Moy, et al., 2012; Keeble, Banerjee, Ferla, Reddington, Anuar, & Howarth, 2017;

50 Bedbrook, Kato, Ravindra Kumar, Lakshmanan, Nath, Sun, et al., 2015). In this chapter we
51 describe methods and principles to design and generate successful SpyTag/SpyCatcher
52 constructs. There are various other approaches for covalent coupling of proteins with other
53 proteins, which we have recently summarized (Banerjee & Howarth, 2018).

54 The CnaB2 domain of the *Streptococcus pyogenes* fibronectin-binding adhesin FbaB
55 spontaneously forms an intramolecular isopeptide bond to stabilize the protein (Hagan,
56 Björnsson, McMahon, Schomburg, Braithwaite, Bühl, et al., 2010). Our group split this domain
57 into two parts: the SpyCatcher protein and the SpyTag peptide (Figure 1B) (Zakeri et al., 2012).
58 Upon mixing together, the amide bond between Lys and Asp spontaneously reconstitutes,
59 enabling irreversible linking of proteins fused to the SpyCatcher and SpyTag (Figure 2A).
60 Subsequently, rational design and directed evolution produced SpyCatcher002 and SpyTag002
61 (Figure 2B), with an order of magnitude faster reactivity, so reacting to completion even at low
62 (100 nM) protein concentrations (Figure 2B) (Keeble et al., 2017). The sequence relationships
63 between the most common versions of SpyTag/SpyTag002 and SpyCatcher/SpyCatcher002 in
64 the published literature are shown in Figure 2C, including SpyCatcher versions with truncations
65 at each terminus (Li, Fierer, Rapoport, & Howarth, 2014).

66 SpyTag/SpyCatcher can produce constructs of non-linear and unprecedented topologies
67 (Sun, Zhang, Mahdavi, Arnold, & Tirrell, 2014; Zhang, Sun, Tirrell, & Arnold, 2013; Wang,
68 & Zhang, 2016) and can be used orthogonally with other coupling technologies, such as
69 HaloTag or streptavidin (Peschke, Rabe, & Niemeyer, 2017; Fairhead, Veggiani, Lever, Yan,
70 Mesner, Robinson, et al., 2014). SpyTag/SpyCatcher reactions can couple proteins together
71 with high specificity in biological environments including bacterial outer-membranes (Keeble
72 et al. 2017; Peschke et al., 2017), the mammalian cytosol (Zakeri et al., 2012; Hinrichsen, Lenz,
73 Edwards, Miller, Mochrie, Swain, et al., 2017), biofilms (Nguyen, Botyanszki, Tay, & Joshi,
74 2014), the mammalian plasma membrane (Zakeri et al., 2012), and living *Caenorhabditis*
75 *elegans* (Bedbrook et al., 2015).

76 SpyTag/SpyCatcher reactions have a wide-spread use in assembling complexes,
77 enabling the combination of properties of one protein with the protein to which it is covalently
78 coupled (Figure 3). Libraries of antigen-specific binding reagents (DARPs, nanobodies etc.)
79 fused to SpyTag and libraries of detection proteins (fluorescent proteins, reporter enzymes, or
80 toxins) fused to SpyCatcher (Figure 3A) have been created as part of a “Portable, On-Demand
81 Biomolecular Manufacturing” platform (Pardee, Slomovic, Nguyen, Lee, Donghia, Burrill, et
82 al. 2016). Virus-like particles (VLPs) fused to SpyCatcher have been used to create “Plug-and-
83 display” immunogens by multivalently displaying SpyTagged vaccine candidates, to accelerate
84 vaccine generation (Figure 3B) (Brune & Howarth, 2018). Intracellular super-resolution
85 imaging reagents for mammalian cell microscopy have been generated: Cys-SpyCatcher was
86 conjugated with maleimide-Alexa Fluor 647 and added to fixed HEK293T cells expressing
87 cellular components fused to SpyTag (Figure 3C) (Pessino, Citron, Feng, & Huang, 2017).
88 SpyTag-fusions were also detected with high sensitivity in Western blot by Alexa Fluor 647-
89 SpyCatcher, since the low affinity of antibodies detecting conventional peptide tags can often
90 be limiting (Figure 3D) (Dovala, Sawyer, Rath, & Metzger, 2016).

91 Improving the coordination of enzyme function has been a long-standing challenge in
92 biotechnology and synthetic biology. Genetic fusions linking together different enzymes can
93 be successful but can often lead to misfolding and are restricted in the relative spatial
94 orientation of the active sites (Pröschel, Detsch, Boccaccini, & Sonnewald, 2015). Many
95 peptide:protein interactions have been employed to connect enzymes, but stability and
96 specificity of these contacts has often been limiting (Pröschel et al., 2015). Therefore, the
97 simple and irreversible linkage between SpyTag and SpyCatcher can make a contribution to
98 enzyme organization. Particular applications so far include cyclizing enzymes to improve their
99 thermal resilience (Figure 4A). This was initially demonstrated for β -lactamase, where

100 SpyTag- β -lactamase-SpyCatcher retained solubility and activity following boiling (Schoene,
101 Fierer, Bennett, & Howarth, 2014). This “SpyRing” approach has since been extended to
102 luciferase, phytase, glucanase and trehalose synthase (Si, Xu, Jiang, & Huang, 2016; Schoene,
103 Bennett, & Howarth, 2016a; Gilbert, Howarth, Harwood, & Ellis, 2017; Schoene, Bennett, &
104 Howarth, 2016b; Wang, Wang, Wang, Zhang, Wu, & Zhang, 2016; Xu, Xu, Huang, & Jiang,
105 2018). SpyTag has also been used in covalent modification of biofilms to make “living
106 materials” with controlled mechanical and catalytic functions (Figure 4B) (Nguyen et al. 2014;
107 Botyanszki, Tay, Nguyen, Nussbaumer, & Joshi, 2015). SpyTag was applied to the intracellular
108 delivery of enzymes by modular linkage to cell penetrating peptides (Figure 4C) (Hoffman,
109 Milech, Juraja, Cunningham, Stone, Francis, et al., 2018; Stone, Heinrich, Juraja, Satiaputra,
110 Hall, Anastasas, et al., 2018). SpyTag also facilitated construction of multimerized enzyme
111 assemblies either using VLPs (Röder, Fischer, & Commandeur, 2017) (as in Figure 3B) or
112 other biological nanoreactors (Figure 4D) (Alves, Turner, Daniele, Oh, Medintz, & Walper,
113 2017; Pröschel, et al., 2015; Giessen, & Silver, 2016; Yin, Guo, Liu, Zhang, & Feng, 2018).
114 Such complexes also enable a scaffolding function, organizing proteases for amplification
115 towards cancer diagnosis (Stein, Nabi, & Alexandrov, 2017), as well as immobilizing enzymes
116 for robust nanopore DNA sequencing devices (Stranges, Palla, Kalachikov, Nivala, Dorwart,
117 Trans, et al., 2016).

118 We have assembled a more complete list of publications and patents using
119 SpyTag/SpyCatcher technology at the SpyInfo webpage
120 (www.bioch.ox.ac.uk/howarth/info.htm). The webpage also contains the papers applying other
121 spontaneous isopeptide bond-forming systems (Zakeri et al., 2012; Abe, Wakabayashi,
122 Yonemura, Yamada, Goto, & Kamiya, 2013). The first split pair was isopeptag/Pilin-C, but
123 pilin-C is much larger than SpyCatcher and reacts much slower (Zakeri & Howarth, 2010).
124 SnoopTag/SnoopCatcher results from the engineering of a D4 domain of the RrgA protein from
125 *Streptococcus pneumoniae*, reacting orthogonally (with no cross-reactivity) to
126 SpyTag/SpyCatcher (Veggiani, Nakamura, Brenner, Gayet, Yan, Robinson, et al., 2016).
127 Further engineering of the CnaB2 domain produced SpyLigase, while SnoopLigase was
128 generated from the RrgA D4 domain (Fierer, Veggiani, & Howarth, 2014; Buldun, Jean,
129 Bedford, & Howarth, 2018). These ligases join two peptides (formed from parts of the original
130 domains) together via isopeptide bonds. However, the speed of reaction of these ligases and
131 their activity with low concentration of target protein is worse than for SpyTag/SpyCatcher
132 ligation.

133 The procedures outlined below should help to avoid potential pitfalls, as well as
134 integrating the insight that is now available from the validation of a wide range of SpyTag and
135 SpyCatcher fusions in different organisms, compartments and protein contexts.

136

137 **2. SpyDesign – construction of successful SpyTag/SpyCatcher reagents**

138

139 2.1 SpyBank database:

140 SpyBank is an online database that we have compiled of amino acid sequences of SpyTag- or
141 SpyCatcher-fusions available from published papers or patents by different academics or
142 companies. Example entries are shown in Table 1. As of September 2018, there are more than
143 400 sequence entries, available for download from our webpage
144 (www.bioch.ox.ac.uk/howarth/info.htm). In addition to listing corresponding author and
145 citation, SpyBank contains important experimental design information on the expression host,
146 cellular compartment, where the protein was fused, which version of SpyCatcher or SpyTag
147 was used, as well as the amino acid sequence of the constructs used (where available). The
148 plasmids for basic SpyCatcher and SpyTag constructs are available from the Addgene plasmid
149 repository (www.addgene.org): SpyCatcher (#35044); Δ N1 Δ C2SpyCatcher (#87376);

150 SpyTag-maltose binding protein (MBP) (#35050); AviTag-SpyCatcher (#72326);
151 SpyCatcher002 (#102827); SpyTag002-MBP (#102831).

152 SpyBank reveals that *Escherichia coli* is by far the most common system for expression
153 of SpyTag/SpyCatcher fusions. However, a range of other species have been successfully used.
154 Other bacteria used for expression were *Bacillus subtilis*, *Lactococcus lactis*, and *Salmonella*
155 *Typhimurium*. Among eukaryotes, expression has been performed in *Saccharomyces*
156 *cerevisiae*, *C. elegans*, insect cells (ExpresS2, Sf9, *Trichoplusia ni*), human cell-lines (HeLa,
157 HEK293) and the plant *Nicotiana benthamiana*. Expression has also been performed in cell-
158 free systems (Pardee, et al., 2016). This diversity supports the wide-spread biological
159 compatibility of SpyCatcher and SpyTag.

160 In addition to cytosolic protein expression, SpyTagged proteins have been secreted from
161 HEK293T cells, using signal peptides at the N-terminus of the construct to target for
162 endoplasmic reticulum translocation. Some signal peptides are useful for many proteins, but
163 others are more specific (Kober, Zehe, & Bode, 2013), so trials with different signal peptides
164 may be useful for the highest expression levels. These cells can also be used to express proteins
165 targeted to the membrane. Alternative signal peptides compatible with membrane display of
166 SpyTagged proteins are listed in SpyBank.

167

168 2.2 Construct design:

169 When designing constructs involving SpyTag and SpyCatcher variants, the following
170 considerations should be taken into account:

171

172 (i) Choice of SpyCatcher and SpyTag variant.

173 For N- or C-terminal fusion of SpyCatcher, we would recommend the $\Delta N1$ SpyCatcher
174 construct (Figure 2C) (Li et al., 2014), which gave us the best results in the challenging
175 situation of VLP fusion (Brune, Leneghan, Brian, Ishizuka, Bachmann, Draper, et al. 2016). If
176 the SpyCatcher is to be inserted in an internal protein loop, we suggest $\Delta N1\Delta C2$ SpyCatcher,
177 which was successfully applied for bacterial microcompartments (Hagen, Sutter, Sloan, &
178 Kerfeld, 2018). If reaction speed is limiting, we recommend switching to SpyCatcher002 to
179 accelerate the reaction with SpyTag, especially at low (< 100 nM) protein concentrations
180 (Keeble et al. 2017). We have found that the N-terminal sequence of SpyCatcher expression
181 constructs starting with GAMVD result in a trace amount of side-reaction with the reactive
182 lysine of another SpyCatcher molecule, since this sequence partially resembles the SpyTag
183 sequence (Keeble et al. 2017). During the development of the faster reacting SpyCatcher002,
184 we found that this off-pathway reaction was enhanced, requiring the mutation of the sequence
185 to GAMVT (Keeble et al. 2017). Thus, we recommend also including this mutation in
186 SpyCatcher constructs, as well as ensuring that sequences like this are not used in linker
187 regions.

188 SpyBank shows many examples of SpyTag being used at the N- or C-terminus. SpyTag
189 may also be used in exposed linker regions between protein domains (Zakeri et al., 2012).
190 There are fewer examples of SpyTag being used in a loop within a folded domain (Hagen et
191 al., 2018; Kasaraneni, Chamoun-Emanuelli, Wright, & Chen, 2017; Moon, Bae, Kim, & Kang,
192 2016); optimization may sometimes be required, because SpyTag reacts in an elongated
193 conformation with SpyCatcher (Figure 1B) (Li et al., 2014). SpyTag and SpyTag002 can be
194 used interchangeably but reaction with any SpyCatcher variant will be faster with SpyTag002
195 (Keeble et al., 2017).

196

197 (ii) Choice of fusion site.

198 SpyCatcher and SpyTag can be used equally well on the N- or C-terminus, since the reaction
199 is mediated through side-chains. SpyBank also contains several constructs with more than one

200 SpyTag or more than one SpyCatcher moiety (Zhang et al., 2013; Wieduwild & Howarth,
201 One may prefer a particular terminus because it is distant from a binding site or active
202 site, because previous fusion to other tags has been successful (e.g. to a His₆-tag or fluorescent
203 protein), or because there is lower sequence conservation at that terminus (Chen, Zaro, & Shen,
204 2013). If an initial construct shows sub-optimal activity, it is worth moving SpyCatcher or
205 SpyTag to the opposite terminus, to see if activity is improved (Si et al., 2016).

206 SpyCatcher and SpyTag must be sterically accessible to one another for reaction to
207 occur. This consideration is of particular importance when using large multimeric proteins,
208 where either the N- or C-terminus may point into the core of the protein (Hagen et al., 2018;
209 Brune & Howarth, 2018).

210
211 (iii) Choice of linker.

212 We always insert a linker between SpyTag or SpyCatcher and the protein of interest. Initially
213 we usually try GSGESGSG (Veggiani et al., 2016). Gly/Ser linkers show a good balance of
214 flexibility, solubility and protease resistance (Chen et al. 2013) and we often include a Glu in
215 the spacer to increase hydrophilicity. The linker increases the accessibility of
216 SpyTag/SpyCatcher for faster and higher yielding reaction. The linker also reduces the chance
217 of interference in the structure or function of the fused protein. If a linker has been used on a
218 similar protein in SpyBank, we would suggest copying that linker. If we find slow or
219 incomplete reaction, we will often move to a 9-residue linker, such as GGGSGGGGS
220 (Veggiani et al., 2016). When using ΔN1ΔC2SpyCatcher in an internal loop, GGGSGGS was
221 used on each side (Hagen et al., 2018). With SpyTag in an internal loop, linkers such as GGGGS
222 on both sides have been used successfully in SpyBank (Alves et al., 2017).

223 We suggest avoiding linkers containing Asp or Asn close to the C-terminal side of
224 SpyCatcher. For example, a sequence at the C-terminus of SpyCatcher like ...**AHIGSGDG**...
225 could promote self-reaction of the Asp in bold with the reactive lysine of SpyCatcher (C-
226 terminus of SpyCatcher is underlined). Also, we avoid negatively-charged peptides (e.g. myc
227 tag or C-tag) immediately adjacent to SpyTag, where electrostatic complementarity may slow
228 reaction with SpyCatcher.

229
230 (iv) Codon usage.

231 We have nearly always used the original codons for SpyTag and SpyCatcher from *S. pyogenes*
232 and this usage has not caused problems for *E. coli* expression. Gene design companies or online
233 servers are able to suggest optimized codon usage for any species, but sometimes unpredicted
234 effects can lead to worse expression. For expression in other organisms, it is worth looking in
235 SpyBank to identify previous constructs expressed in that species. For simplicity, SpyBank
236 only shows amino acid sequences, but SpyBank should help users to go to the primary source
237 and find the DNA sequence. An exception that we found is the expression of SpyTag at the N-
238 terminus in *E. coli*, where the issue is not codon frequency but codon complementarity.
239 Secondary structure near the Shine-Dalgarno sequence can greatly reduce protein expression
240 yield. Thus, the sequence needs to be optimized using a Ribosome Binding Calculator (score
241 10,000 or above) to maximize expression levels (Salis 2011). We give here SpyTag DNA
242 sequences for two common promoter systems for bacterial expression:

243
244 T7 vector 5' -gcacacatagtaatggttagacgcctacaagccgacgaag-3'
245 T5 vector 5' -gctcatatcgtcatggttgacgcgtataaaccgaccaa-3'
246 A H I V M V D A Y K P T K

247

248 Our constructs will typically have a glycine immediately after the initiating methionine/formyl
249 methionine, which can help expression, consistent with the N-end rule for protein stability
250 (Varshavsky, 2011).

251

252 2.3 Cellular expression and purification:

253 After creation of the desired expression construct, the plasmid is next transformed into an
254 expression strain. We will not go into detail here on protocols that are standard for any protein
255 but focus on issues specific to SpyTag/SpyCatcher. Our standard Ni-NTA purification protocol
256 is described in detail previously (Howarth & Ting, 2008).

257

258 (i) Bacterial expression. SpyBank reveals that a wide-range of different *E. coli* strains can be
259 used for expression of SpyTag/SpyCatcher fusions. Hence, if you find low expression in one
260 strain, you should try others. Two *E. coli* strains we recommend are BL21 (DE3) RIPL
261 (Agilent) (helping to express proteins with rare codons) and C41 (DE3) (helping expression of
262 toxic proteins) (Miroux & Walker, 1996). *E. coli* BL21 (DE3) transformed with a plasmid
263 encoding Erv1p and DsbC allowed us to express efficiently proteins containing a disulfide bond
264 in the cytosol (Veggiani et al., 2016). Supplementing LB media with 0.8% glucose may reduce
265 leaky expression before induction, which aids growth for toxic proteins (Grossman, Kawasaki,
266 Punreddy, & Osburne, 1998). Alternative growth media such as 2×TY or auto-induction media
267 can also be used with SpyTag/SpyCatcher constructs. After inducing with IPTG at OD₆₀₀ 0.5,
268 we typically grow the cells for a further 4 hours at 30 °C. For most constructs we can clearly
269 see induction by SDS-PAGE with Coomassie staining on the whole cell lysate (Figure 2A).

270 If expression has failed, we will first try an alternative induction temperature (18 °C for
271 16 hours) or a different *E. coli* strain. Purification of His₆-tagged fusions by Ni-NTA is carried
272 out by standard methods (Zakeri et al., 2012) ensuring protease inhibitors are present during
273 cell disruption and initial purification. After elution from affinity chromatography, proteins
274 can be dialysed into the buffer of choice (typically phosphate-buffered saline, PBS: 137 mM
275 NaCl, 2.7 mM KCl, 10 mM Na₂HPO₄, 1.8 mM KH₂PO₄ pH 7.5). Dialysis is especially
276 important after Ni-NTA purification, since high concentrations of imidazole slow down the
277 SpyTag/SpyCatcher reaction. If there is substantial aggregation upon dialysis, we will try a
278 buffer with a pH more than 1 unit from the isoelectric point (pI) of the fusion protein (e.g. 50
279 mM Tris base with the pH adjusted using boric acid, or 50 mM glycine
280 with 25 mM sodium citrate with the pH adjusted using HCl or NaOH).

281 A further round of purification such as gel filtration can be used if required, but many
282 SpyCatcher- or SpyTag-linked proteins are typically pure enough to couple to the binding
283 partner after one step purification (Figure 2A). C-tag purification is also efficient for SpyTag-
284 fusions and may be preferred for vaccine studies (Bruun, Andersson, Draper, & Howarth,
285 2018). For the highest purity, we typically combine Ni-NTA purification with gel filtration
286 chromatography or C-tag purification (Brune et al., 2016).

287 Expression yields of 15-30 mg per liter of culture are typically achieved with
288 SpyCatcher- or SpyTag-fusions, although VLP fusion was more challenging (Bruun et al.,
289 2018). Proteins can be stored at 4 °C overnight or indefinitely in aliquots at -80 °C. Certain
290 fusions are likely to be sensitive to freeze-thaw, but where we have tested SpyCatcher-fusions
291 on vaccine platforms, we found good resilience to freezing or lyophilization (Brune, Buldun,
292 Li, Taylor, Brod, Biswas, et al., 2017; Bruun et al., 2018).

293

294 (ii) Mammalian secretion. Three related mammalian cell-lines have been widely used in
295 SpyBank – HEK293T (adherent), HEK293 FreeStyle and HEK293Expi. Although several
296 SpyTag-containing constructs are reported (with SpyTag at either N- or C-terminus), there are
297 fewer examples in SpyBank of secretion of a SpyCatcher-fusion. The dynamic structure of

298 SpyCatcher may sometimes reduce the efficiency of secretion. Successful published examples
299 include SpyCatcher at the N-terminus of the IgG Fc domain (Alam, Gonzalez, Hill, El-Sayed,
300 Fonge, Barreto et al., 2017) and SpyCatcher linked to a range of antigens for immunization
301 (Thrane, Janitzek, Matondo, Resende, Gustavsson, de Jongh, et al., 2016). It appears more
302 difficult to express SpyCatcher-fusions than SpyTag-fusions in mammalian cells.

303 Expression constructs can be transiently transfected into the cells at mid-confluency
304 using polyethylene imine (PEI) (HEK293T and HEK293 FreeStyle) or ExpiFectamine 293
305 (HEK293Expi). After secretion of the protein into the media for the desired time (typically 3-
306 7 days), the media is removed from the cells and protease inhibitors are added to prevent
307 proteolysis. After a repeated centrifugation to decrease the amount of cell debris, the
308 supernatant should be syringe-filtered (0.45 μ m). Binding buffer should now be added to the
309 filtered supernatant as required for purification: 50 mM Tris•HCl, 300 mM NaCl, pH 7.8 to ¼
310 of total volume. This is important for pH buffering, since the growth medium does not buffer
311 effectively without high CO₂. Given the large volume of cell supernatant produced (100-1,000
312 mL typically), affinity purification (His₆-tag or C-tag) is essential to concentrate the protein
313 and can now proceed as required for the standard protocols.

314

315 **3. Analysis of SpyTag/SpyCatcher covalent coupling reactions**

316

317 3.1 Reaction of components:

318 SpyTag/SpyCatcher reaction readily occurs without requiring any specific anions or cations, at
319 a range of temperatures (4-37 °C), at pH from 4 to 8, in the presence of various detergents
320 (Tween-20, Triton X-100, Nonidet P-40, CHAPS, but not SDS), and even under chaotropic
321 conditions such as 4 M urea (Keeble et al., 2017). This flexibility makes SpyTag/SpyCatcher
322 coupling suited to a wide range of coupling tasks. We typically mix the SpyCatcher- and
323 SpyTag-proteins in a buffer such as PBS pH 7.5 with each partner at 10 μ M and incubate for
324 2 hours at room temperature. Reaction is slower, for example, on the crowded surface of VLPs,
325 where we usually incubate for 16 hours (Brune et al., 2016; Bruun et al., 2018). To ensure one
326 partner is fully reacted, we recommend incubating with one component in 1.5-3 \times excess. Given
327 that the reaction follows second-order kinetics (Zakeri et al., 2012; Keeble et al., 2017), it is
328 not just the ratio but also the absolute concentration which is important for reaction speed.
329 Given the broad tolerance of SpyTag/SpyCatcher reaction described above, it is worth
330 including additives (e.g. Ca²⁺, glycerol, cofactors) likely to stabilize the proteins of interest.

331 When testing new constructs, we recommend using purified SpyCatcher or SpyTag-MBP
332 proteins as positive controls under the same conditions. These positive controls are very helpful
333 for troubleshooting, to determine whether the buffer or protein constructs may be at fault, if
334 the novel protein partners do not react as desired. Negative control constructs are also helpful
335 to validate that any observed effects depend on covalent reaction. Such controls bear a mutation
336 in the reactive residue of SpyTag (SpyTag002 DA-MBP Addgene # 102832) or SpyCatcher
337 (SpyCatcher EQ Addgene # 35045 or SpyCatcher002 EQ Addgene # 102830) (Zakeri et al.,
338 2012; Keeble et al., 2017).

339

340 3.2 Analysis of reaction:

341 (i) SDS-PAGE

342 Formation of covalent SpyTag/SpyCatcher reaction products *in vitro* can be observed and
343 quantified by SDS-polyacrylamide gel electrophoresis (Figure 2A), since the isopeptide bond
344 is stable to boiling in SDS (Zakeri et al., 2012; Keeble et al., 2017). This approach enables
345 convenient quantitation by densitometry, based on either formation of the SpyTag:SpyCatcher
346 conjugate or the depletion of SpyTag or SpyCatcher starting material. Note that the mobility
347 of the SpyTag:SpyCatcher conjugate may be slightly different from the molecular weight

348 because of its branched nature (Zakeri et al., 2012; Schoene et al., 2016) and a second band
349 may be present on SpyCatcher-fusions, as discussed in section 3.2 (ii).

350 (ii) Mass spectrometry

351 Mass spectrometry is helpful to confirm the exact product of SpyTag/SpyCatcher reaction.
352 Isopeptide bond formation for this pair results in loss of H₂O (18 Da). For analysis of the
353 reaction of purified samples, we dialyze into 10 mM ammonium acetate, since the low ionic
354 strength and volatile buffer components assist in obtaining a clean spectrum. A common
355 impurity after *E. coli* expression is a gluconylated adduct (Geoghegan, Dixon, Rosner, Hoth,
356 Lanzetti, Borzilleri et al., 1999), but we have never experienced functional consequences of
357 this impurity.

358 (iii) Fluorescence microscopy

359 The specificity and efficiency of *in vivo* reaction of SpyTag/SpyCatcher can be examined by
360 microscopy. The first step is labeling with fluorescent proteins fused to the SpyCatcher or
361 SpyTag construct and using microscopy to detect the cellular distribution of the target protein.
362 This approach was used to demonstrate that SpyTag-Channelrhodopsin-mCherry constructs
363 can react with SpyCatcher-GFP in *C. elegans* (Bedbrook et al., 2015).

364 (iv) Western blotting

365 Western blotting was performed on lysate from cells expressing SpyCatcher or SpyTagged
366 proteins, with reaction occurring upon staining of the transferred membrane (Dovala et al.,
367 2016). Western blotting can also be used to follow reaction occurring on living cells, such as
368 to show that biotinylated-AviTag-SpyTag002-MBP reacted specifically with the bacterial
369 outer membrane-displayed Intimin-myc tag-SpyCatcher002, using Streptavidin-Horse Radish
370 Peroxidase (to detect the biotinylated protein) or an anti-myc antibody (followed by secondary
371 antibody-HRP) to follow the total pool of cell-surface Intimin (Keeble et al., 2017).

372

373 3.3 Conjugate purification:

374 After the desired reaction time, unreacted SpyTag or SpyCatcher components may be purified
375 from the covalent complexes, using size-exclusion chromatography, spin-filtration or dialysis
376 (Brune et al., 2016). When there is a large size difference between the two partners (e.g.
377 SpyTag-antigen separation from antigen-decorated VLP), we found dialysis to be a simple and
378 efficient approach, leading to minimal dilution of the sample (Brune et al., 2016).

379

380 **3. Concluding Remarks**

381 We have described here guidelines on how to design and purify constructs to use
382 SpyTag/SpyCatcher for covalent coupling of proteins, based on our own experience and the
383 results of many other groups, as compiled in SpyBank. It is relatively simple to generate
384 functional SpyTag or SpyCatcher constructs in a range of cellular systems. Reaction is typically
385 efficient and selective either *in vitro* or at the surface of cells. There are few examples of
386 SpyTag/SpyCatcher reaction inside living cells, so it will be important to validate this
387 application in future work, perhaps with new iterations of Tag/Catcher pairs. Future
388 development should also seek to establish the principles for efficient use of
389 SpyTag/SpyCatcher in protein loops and efficient secretion of SpyCatcher-fusions from
390 mammalian cells. Combining SpyTag/SpyCatcher with related technologies such as
391 SnoopCatcher (Veggiani et al., 2016) and SnoopLigase (Buldun et al., 2018) will also provide
392 further opportunities for creating novel protein architectures, signaling teams (Veggiani et al.,
393 2016) and immune stimulants (Brune et al., 2017).

394

395 **Acknowledgements**

396 Funding was provided by the European Research Council (ERC-2013-CoG 615945-
397 PeptidePadlock).

398

399 **Conflicts of interest**

400 M.H. and A.H.K. are authors on a patent application covering sequences for enhanced
401 isopeptide bond formation (UK Intellectual Property Office 1706430.4). M.H. is an author on
402 a patent for isopeptide bond formation (EP2534484) and a SpyBiotech co-founder, shareholder
403 and consultant.

404

405 **References**

406

407 Abe, H., Wakabayashi, R., Yonemura, H., Yamada, S., Goto, M., & Kamiya, N. (2013). Split
408 Spy0128 as a potent scaffold for protein cross-linking and immobilization. *Bioconjug*
409 *Chem.* 24(2), 242-50.

410 Alam, M.K., Gonzalez, C., Hill, W., El-Sayed, A., Fonge, H., Barreto, K. et al. (2017).
411 Synthetic Modular Antibody Construction by Using the SpyTag/SpyCatcher Protein-
412 Ligase System. *ChemBioChem.* 18(22), 2217-2221.

413 Alves, N.J., Turner, K.B., Daniele, M.A., Oh, E., Medintz, I.L., & Walper, S.A. (2017).
414 Bacterial Nanobioreactors—Directing Enzyme Packaging into Bacterial Outer
415 Membrane Vesicles. *ACS Appl Mater Interfaces.* 7(44), 24963-24972.

416 Banerjee, A., & Howarth, M. (2018). Nanoteamwork: covalent protein assembly beyond duets
417 towards protein ensembles and orchestras. *Curr Opin Biotechnol.* 51, 16-23.

418 Bedbrook, C.N., Kato, M., Ravindra, Kumar, S., Lakshmanan, A., Nath, R.D., Sun, F. et al.
419 (2015). Genetically Encoded Spy Peptide Fusion System to Detect Plasma Membrane-
420 Localized Proteins In Vivo. *Chem Biol.* 22(8), 1108-1121.

421 Botyanszki, Z., Tay, P.K., Nguyen, P.Q., Nussbaumer, M.G., & Joshi, N.S. (2015). Engineered
422 catalytic biofilms: Site-specific enzyme immobilization onto E. coli curli nanofibers.
423 *Biotechnol Bioeng.* 112(10), 2016-2024.

424 Brune, K.D., Leneghan, D.B., Brian, I.J., Ishizuka, A.S., Bachmann, M.F., Draper, S.J. et al.
425 (2016). Plug-and-Display: decoration of Virus-Like Particles via isopeptide bonds for
426 modular immunization. *Sci Rep.* 6, 19234.

427 Brune, K.D., Buldun, C.M., Li, Y., Taylor, I.J., Brod, F., Biswas, S. et al. (2017). Dual Plug-
428 and-Display Synthetic Assembly Using Orthogonal Reactive Proteins for Twin Antigen
429 Immunization. *Bioconjug Chem.* 28(5), 1544-1551.

430 Brune, K.D., & Howarth, M. (2018). New Routes and Opportunities for Modular Construction
431 of Particulate Vaccines: Stick, Click, and Glue. *Front Immunol.* 9, 1432.

432 Bruun, T.U.J., Andersson, A.C., Draper, S.J., & Howarth, M. (2018). Engineering a Rugged
433 Nanoscaffold To Enhance Plug-and-Display Vaccination. *ACS Nano.* doi:
434 10.1021/acsnano.8b02805.

435 Buldun, C.M., Jean, J.X., Bedford, M.R., & Howarth, M. (2018) SnoopLigase Catalyzes
436 Peptide-Peptide Locking and Enables Solid-Phase Conjugate Isolation. *J Am Chem Soc.*
437 140(8), 3008-3018.

438 Chen, X., Zaro, J.L., & Shen, W.C. (2013). Fusion protein linkers: property, design and
439 functionality. *Adv Drug Deliv Rev.* 65(10), 1357-1369.

440 Dovala, D. Sawyer, W.S. Rath, C.M. Metzger, L.E. 4th. (2016). Rapid analysis of protein
441 expression and solubility with the SpyTag-SpyCatcher system. *Protein Expr Purif.* 117,
442 44-51.

443 Fairhead, M., Veggiani, G., Lever, M., Yan, J., Mesner, D., Robinson, C.V. et al. (2014).
444 SpyAvidin hubs enable precise and ultrastable orthogonal nanoassembly. *J Am Chem*
445 *Soc.* 136(35), 12355-12363.

446 Fierer, J.O., Veggiani, G., & Howarth, M. (2014). SpyLigase peptide-peptide ligation
447 polymerizes affibodies to enhance magnetic cancer cell capture. *Proc Natl Acad Sci U*
448 *S A.* 111(13), E1176-1181.

449 Geoghegan, K.F., Dixon, H.B., Rosner, P.J., Hoth, L.R., Lanzetti, A.J., Borzilleri, K.A. et al.
450 (1999). Spontaneous alpha-N-6-phosphogluconoylation of a "His tag" in *Escherichia*
451 *coli*: the cause of extra mass of 258 or 178 Da in fusion proteins. *Anal Biochem.*
452 267(1),169-184.

453 Giessen, T.W., & Silver, P.A. (2016). A Catalytic Nanoreactor Based on in Vivo Encapsulation
454 of Multiple Enzymes in an Engineered Protein Nanocompartment. *ChemBioChem.*
455 17(20), 1931-1935.

456 Gilbert, C., Howarth, M., Harwood, C.R., & Ellis, T. (2017). Extracellular Self-Assembly of
457 Functional and Tunable Protein Conjugates from *Bacillus subtilis*. *ACS Synth Biol.*
458 6(6), 957-967.

459 Grossman, T.H., Kawasaki, E.S., Punreddy, S.R., & Osburne M.S. (1998). Spontaneous
460 cAMP-dependent derepression of gene expression in stationary phase plays a role in
461 recombinant expression instability. *Gene.* 209(1-2), 95-103.

462 Hagan, R.M., Björnsson, R., McMahon, S.A., Schomburg, B., Braithwaite, V., Bühl, M. et al.
463 (2010). NMR spectroscopic and theoretical analysis of a spontaneously formed Lys-
464 Asp isopeptide bond. *Angew Chem Int Ed Engl.* 49(45), 8421-8425

465 Hagen, A., Sutter, M., Sloan, N., & Kerfeld, C.A. (2018). Programmed loading and rapid
466 purification of engineered bacterial microcompartment shells. *Nat Commun.* 9(1),
467 2881.

468 Hinrichsen, M., Lenz, M., Edwards, J.M., Miller, O.K., Mochrie, S.G.J. Swain P.S. et al.
469 (2017). A new method for post-translationally labeling proteins in live cells for
470 fluorescence imaging and tracking. *Protein Eng Des Sel.* 30(12), 771-780.

471 Hoffmann, K., Milech, N., Juraja, S.M., Cunningham, P.T., Stone, S.R., Francis, R.W. et al.
472 (2018). A platform for discovery of functional cell-penetrating peptides for efficient
473 multi-cargo intracellular delivery. *Sci Rep.* 8(1), 12538.

474 Howarth, M., & Ting, A.Y. (2008). Imaging proteins in live mammalian cells with biotin ligase
475 and monovalent streptavidin. *Nat Protoc.* 3(3), 534-545.

476 Kasaraneni, N., Chamoun-Emanuelli, A.M., Wright, G., & Chen, Z. (2017). Retargeting
477 Lentiviruses via SpyCatcher-SpyTag Chemistry for Gene Delivery into Specific Cell
478 Types. *mBio.* 8(6), e01860-17.

479 Keeble, A.H., Banerjee, A., Ferla, M.P., Reddington, S.C., Anuar, I.N.A.K., & Howarth, M.
480 (2017). Evolving Accelerated Amidation by SpyTag/SpyCatcher to Analyze
481 Membrane Dynamics. *Angew Chem Int Ed Engl.* 56(52), 16521-16525.

482 Kober, L., Zehe, C., & Bode, J. (2013). Optimized signal peptides for the development of high
483 expressing CHO cell lines. *Biotechnol Bioeng.* 110(4), 1164-1173.

484 Li, L., Fierer, J.O., Rapoport, T.A., & Howarth, M. (2014). Structural analysis and optimization
485 of the covalent association between SpyCatcher and a peptide Tag. *J Mol Biol.* 426(2),
486 309-317.

487 Miroux, B., & Walker, J.E. (1996) Over-production of proteins in *Escherichia coli*: mutant
488 hosts that allow synthesis of some membrane proteins and globular proteins at high
489 levels. *J Mol Biol.* 260, 289-298.

490 Moon, H., Bae, Y., Kim, H., & Kang, S. (2016). Plug-and-playable fluorescent cell imaging
491 modular toolkits using the bacterial superglue, SpyTag/SpyCatcher. *Chem Commun*
492 *(Camb).* 52(97), 14051-14054.

493 Nguyen, P.Q., Botyanszki, Z., Tay, P.K., & Joshi, N.S. (2014). Programmable biofilm-based
494 materials from engineered curli nanofibres. *Nat Commun.* 5, 4945.

495 Pardee, K, Slomovic, S., Nguyen, P.Q., Lee, J.W., Donghia, N., Burrill, D et al. (2016).
496 Portable, On-Demand Biomolecular Manufacturing. *Cell*. 167(1), 248-259.

497 Peschke, T., Rabe, K.S., & Niemeyer, C.M. (2017). Orthogonal Surface Tags for Whole-Cell
498 Biocatalysis. *Angew Chem Int Ed Engl*. 56(8), 2183-2186.

499 Pessino, V., Citron, Y.R., Feng, S., Huang, B. (2017). Covalent Protein Labeling by SpyTag-
500 SpyCatcher in Fixed Cells for Super-Resolution Microscopy. *ChemBioChem*. 18(15),
501 1492-1495.

502 Pröschel, M., Detsch, R. Boccaccini, A.R. & Sonnewald, U. (2015). Engineering of Metabolic
503 Pathways by Artificial Enzyme Channels. *Front Bioeng Biotechnol*. 3, 168.

504 Röder, J., Fischer, R., & Commandeur, U. (2017). Engineering Potato Virus X Particles for a
505 Covalent Protein Based Attachment of Enzymes. *Small*. 13(48), 1702151.

506 Salis, H.M. (2011). The ribosome binding site calculator. *Methods Enzymol*. 498:19-42.

507 Schoene, C., Fierer, J.O., Bennett, S.P., & Howarth, M. (2014). SpyTag/SpyCatcher
508 cyclization confers resilience to boiling on a mesophilic enzyme. *Angew Chem Int Ed
509 Engl*. 53(24), 6101-6104.

510 Schoene, C., Bennett, S.P., & Howarth M. (2016). SpyRing interrogation: analyzing how
511 enzyme resilience can be achieved with phytase and distinct cyclization chemistries.
512 *Sci Rep*. 6, 21151.

513 Schoene, C., Bennett, S.P., & Howarth, M. (2016). SpyRings Declassified: A Blueprint for
514 Using Isopeptide-Mediated Cyclization to Enhance Enzyme Thermal Resilience.
515 *Methods Enzymol*. 580, 149-167.

516 Si, M., Xu, Q., Jiang, L., & Huang, H. (2016). SpyTag/SpyCatcher Cyclization Enhances the
517 Thermostability of Firefly Luciferase. *PloS One*. 11, e0162318.

518 Stein, V., Nabi, M., & Alexandrov, K. (2017). Ultrasensitive Scaffold-Dependent Protease
519 Sensors with Large Dynamic Range. *ACS Synth Biol*. 6(7), 1337-1342.

520 Stone, S.R., Heinrich, T., Juraja, S.M., Satiaputra, J.N., Hall, C.M., Anastasas, M. et al. (2018).
521 β -Lactamase Tools for Establishing Cell Internalization and Cytosolic Delivery of Cell
522 Penetrating Peptides. *Biomacromolecules*. 8(3), E51.

523 Stranges, P.B., Palla, M., Kalachikov, S., Nivala, J, Dorwart, M., Trans, A. et al. (2016).
524 Design and characterization of a nanopore-coupled polymerase for single-molecule
525 DNA sequencing by synthesis on an electrode array. *Proc Natl Acad Sci U S A*. 113(44),
526 E6749-E6756.

527 Sun, F., Zhang, W.B., Mahdavi, A., Arnold, F.H., & Tirrell, D.A. (2014). Synthesis of bioactive
528 protein hydrogels by genetically encoded SpyTag-SpyCatcher chemistry. *Proc Natl
529 Acad Sci U S A*. 111(31), 11269-11274.

530 Thrane, S., Janitzek, C.M., Matondo, S., Resende, M., Gustavsson, T., de Jongh, W.A. et al.
531 (2016). Bacterial superglue enables easy development of efficient virus-like particle
532 based vaccines. *J Nanobiotechnology*. 14, 30.

533 Varshavsky, A. (2011). The N-end rule pathway and regulation by proteolysis. *Protein Sci*.
534 20(8), 1298-1345.

535 Veggiani, G., Nakamura, T., Brenner, M.D., Gayet, R.V., Yan, J., Robinson, C.V. et al. (2016).
536 Programmable polyproteins built using twin peptide superglues. *Proc Natl Acad Sci
537 U S A*. 113(5), 1202-1207.

538 Wang, X.W., & Zhang, W.B. (2016). Cellular Synthesis of Protein Catenanes. *Angew Chem
539 Int Ed Engl*. 55(10), 3442-3446.

540 Wang, X.W., & Zhang, W.B. (2018). Chemical Topology and Complexity of Protein
541 Architectures. *Trends Biochem Sci*. doi: 10.1016/j.tibs.2018.07.001

542 Wang, R., Yang, Z., Luo, J., Hsing, I.M., & Sun, F. (2017). B12-dependent photoresponsive
543 protein hydrogels for controlled stem cell/protein release. *Proc Natl Acad Sci U S A*.
544 114(23), 5912-5917.

545 Wang, J., Wang, Y., Wang, X., Zhang, D., Wu, S., & Zhang, G. (2016). Enhanced thermal
546 stability of lichenase from *Bacillus subtilis* 168 by SpyTag/SpyCatcher-mediated
547 spontaneous cyclization. *Biotechnol Biofuels*. 9, 79.

548 Wieduwild, R., & Howarth, M. (2018). Assembling and decorating hyaluronan hydrogels with
549 twin protein superglues to mimic cell-cell interactions. *Biomaterials*. 180, 253-264.

550 Xu, C., Xu, Q., Huang, H., & Jiang, L. (2018). Enhancing the stability of trehalose synthase
551 via SpyTag/SpyCatcher cyclization to improve its performance in industrial
552 biocatalysts. *Biosci Biotechnol Biochem*. 82(9), 1473-1479.

553 Yin, L., Guo, X., Liu, L., Zhang, Y., & Feng, Y. (2018). Self-Assembled Multimeric-Enzyme
554 Nanoreactor for Robust and Efficient Biocatalysis. *ACS Biomater Sci Eng*. 4(6), 2095–
555 2099.

556 Zakeri, B., & Howarth, M. (2010). Spontaneous intermolecular amide bond formation between
557 side chains for irreversible peptide targeting. *J Am Chem Soc*. 132(13), 4526-4527.

558 Zakeri, B., Fierer, J.O., Celik, E., Chittock, E.C., Schwarz-Linek, U., Moy, V.T. et al. (2012).
559 Peptide tag forming a rapid covalent bond to a protein, through engineering a bacterial
560 adhesin. *Proc Natl Acad Sci U S A.*, 109(12), E690-697.

561 Zhang, W.B. Sun, F. Tirrell, D.A. & Arnold, F.H. (2013). Controlling macromolecular
562 topology with genetically encoded SpyTag-SpyCatcher chemistry. *J Am Chem Soc*.
563 135(37), 13988-13997.

564

565

566

567

568

569

570

571

572

573

574

575

576

577

578

579 .

580

581

582

583

584 **Figure legends**

585

586 **Figure 1:** Principle of SpyTag/SpyCatcher system. **A** Scheme depicting the spontaneous
587 amidation reaction of a lysine side-chain on SpyCatcher to the side-chain of an aspartic acid
588 on SpyTag to form an isopeptide bond. **B** Cartoon illustrating how the CnaB2 domain of FbaB
589 was split and engineered to generate a protein partner, SpyCatcher, reactive with the SpyTag
590 peptide.

591

592 **Figure 2:** SpyTag/SpyCatcher purification and reactivity. **A** SpyTag/SpyCatcher purification.
593 16% SDS-PAGE with Coomassie staining showing post-induction cell lysate for
594 SpyCatcher002 (lane 2) and SpyTag002-MBP (lane 3) expressed in *E. coli*, illustrating high
595 expression levels. Also shown are purified SpyCatcher002 (lane 4), purified SpyTag002-MBP
596 (lane 5), and SpyCatcher002 mixed with SpyTag002-MBP (lane 6); each at 5 μ M in PBS pH
597 7.5 at 25 °C for 1 hr. **B** Increased rate of SpyTag002/SpyCatcher002 reaction. Densitometry
598 from SDS-PAGE for isopeptide bond formation between SpyTag002-MBP and
599 SpyCatcher002 (black) or SpyTag-MBP and SpyCatcher (gray) at 0.1 μ M (top) or 10 μ M
600 (bottom) in succinate-phosphate-glycine buffer at 25 °C. Error bars represent mean \pm SD from
601 triplicates (some error bars are too small to be visible). Data adapted from (Keeble et al., 2017).
602 **C** Amino acid sequence of variants of SpyTag (top) or SpyCatcher (bottom).

603

604 **Figure 3:** Examples of non-enzymatic uses of SpyTag/SpyCatcher. **A** On-Demand
605 Biomolecular Manufacturing platform, using *in vitro* transcription/translation and
606 SpyTag/SpyCatcher to multiplex binding and detection reagents. **B** Plug-and-Display
607 vaccination platform to facilitate decoration of VLPs. **C** Super-resolution cellular imaging with
608 dye-labeled SpyCatcher. **D** Schematic of Western blot detection using Alexa Fluor 647 dye
609 coupled to SpyCatcher.

610

611 **Figure 4:** Examples of enzymatic uses of SpyTag/SpyCatcher. **A** Cyclization of enzymes to
612 improve thermal resilience, showing a cartoon of SpyTag- β -lactamase-SpyCatcher. **B**
613 Production of enzymatic bacterial biofilms. **C** Attachment of chemically-synthesized cell
614 penetrating peptides to enzymes, promoting delivery of functional enzyme intracellularly.
615 CCF2-AM is a membrane-permeable dye which is de-esterified by esterases in the cytosol to
616 give CCF2. Cleavage by cytosolic β -lactamase changes CCF2's fluorescent spectrum. **D**
617 Biological nanoreactors through formation of a covalently-linked enzyme network from a
618 dimeric cytochrome P450 monooxygenase and a tetrameric glucose dehydrogenase, adapted
619 from (Yin et al., 2018).

620

621 **Table 1:** SpyBank sample entries.

622

Figure 1

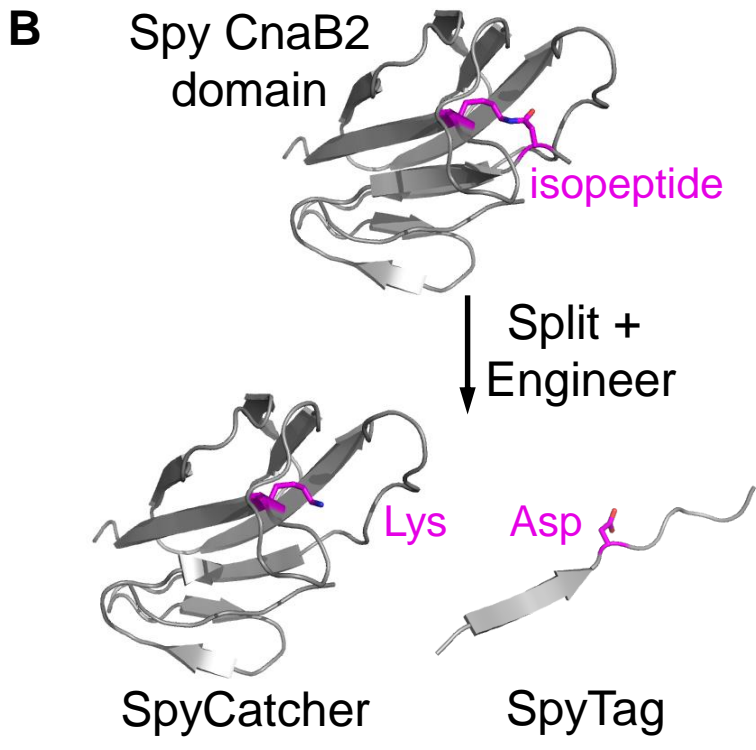
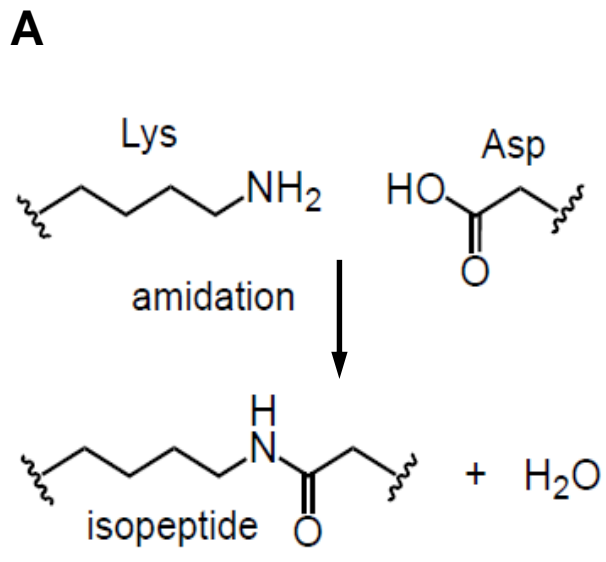
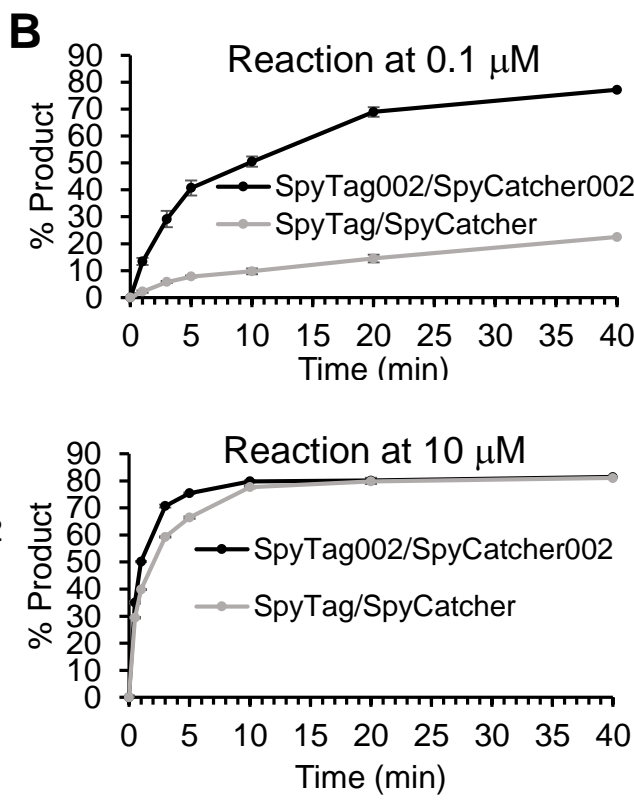
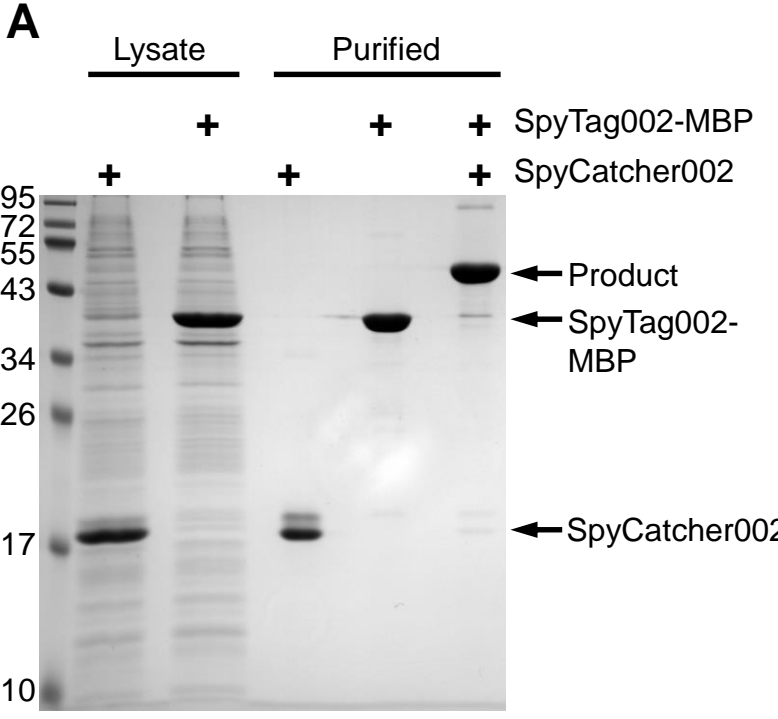


Figure 2



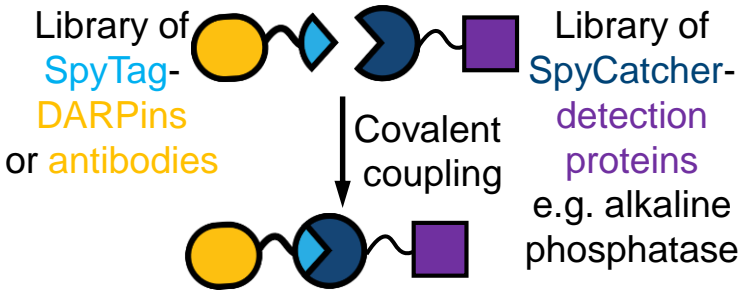
C

SpyTag	-AHIVMVDAYKPTK
SpyTag002	VPTIVMVDAYK R YK
SpyCatcher	VDTLSGLSSEQGQSGDMTIEEDSATHIKFSKRDEDGKELAGATMELRDSSGKTISTWISD
SpyCatcher002	V T TLSGLS G EQ G P S GDMT T EEDSATHIKFSKRDEDG R ELAGATMELRDSSGKTISTWISD
Δ N1SpyCatcher	-----DSATHIKFSKRDEDGKELAGATMELRDSSGKTISTWISD
Δ N1 Δ C2SpyCatcher	-----DSATHIKFSKRDEDGKELAGATMELRDSSGKTISTWISD
SpyCatcher	GQVKDFYLYPGKYTFVETAAPDGYEVATAITFTVNEQGQVTVNGKATKGDAHI
SpyCatcher002	G H VKDFYLYPGKYTFVETAAPDGYEVATAITFTVNEQGQVTVNG E ATKGDA H T
Δ N1SpyCatcher	GQVKDFYLYPGKYTFVETAAPDGYEVATAITFTVNEQGQVTVNGKATKGDAHI
Δ N1 Δ C2SpyCatcher	GQVKDFYLYPGKYTFVETAAPDGYEVATAITFTVNEQGQVTVNG-----

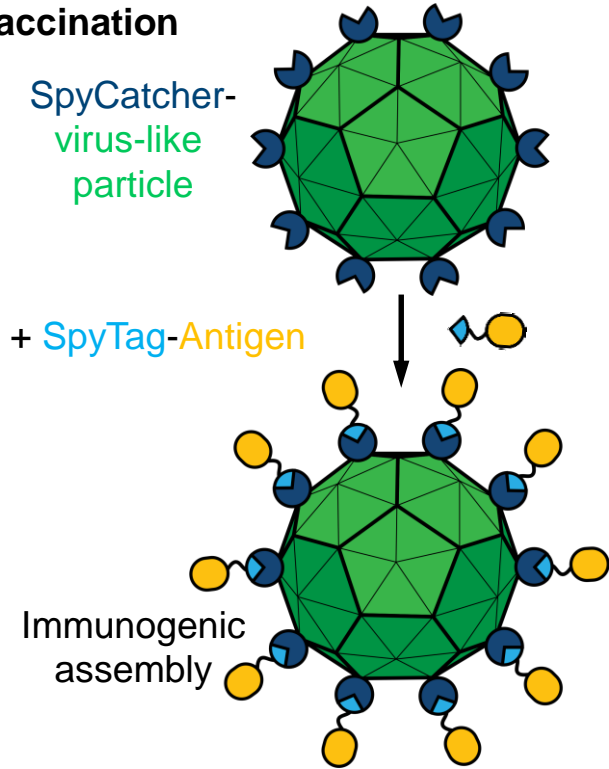
Figure 3

A Multiplexed detection

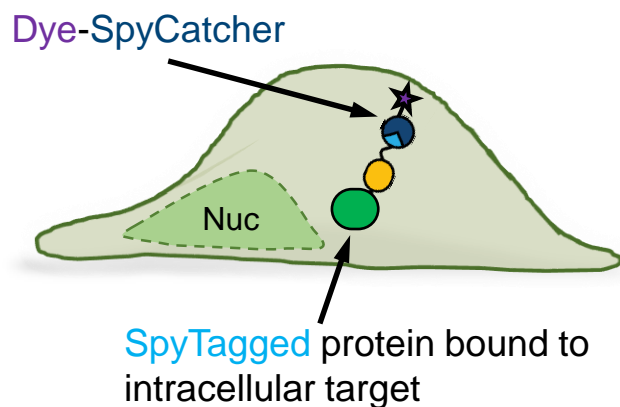
Mix cell-free reactions



B Vaccination



C Super-resolution localization of mammalian intracellular proteins



D Western blot detection

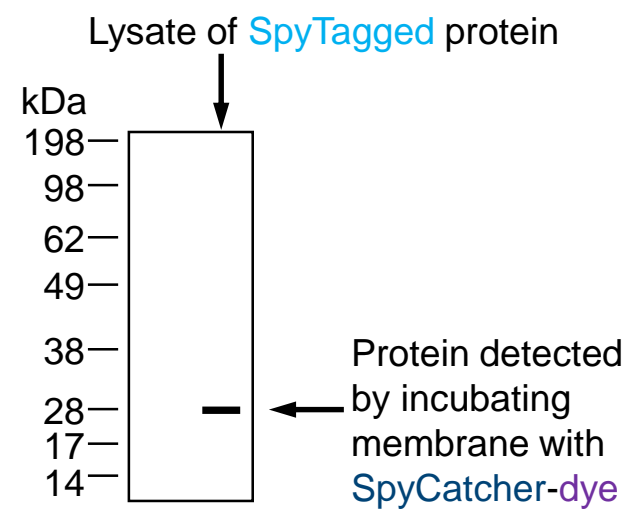
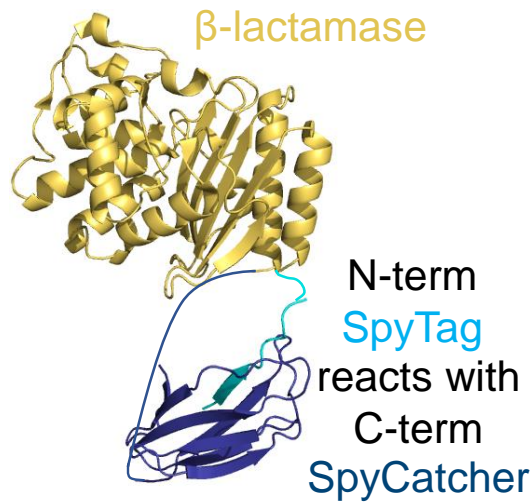


Figure 4

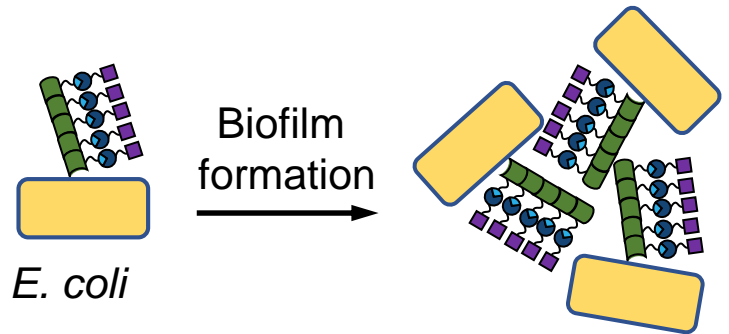
A Enzyme cyclization for resilience



B Catalytic biofilm formation

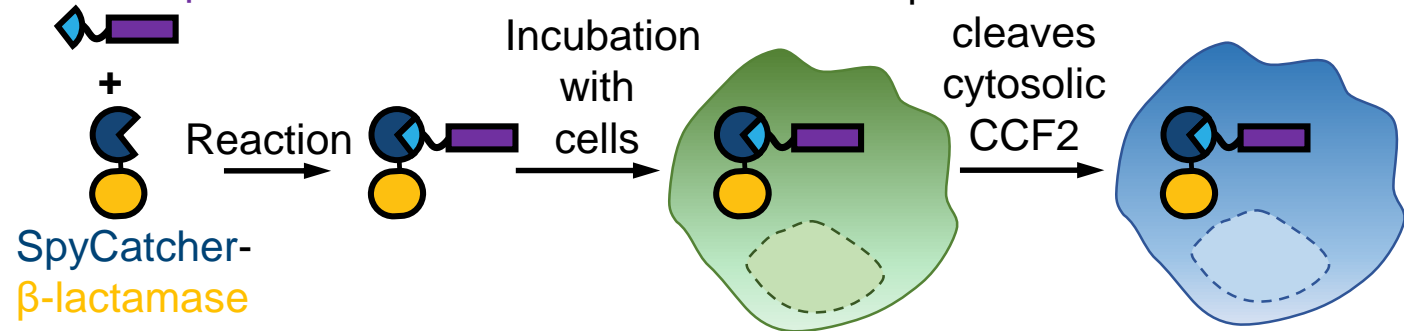
SpyTag-CsgA form curli that react with added SpyCatcher-Enzyme

Biofilm with stabilized enzyme activity



C Enzyme delivery to intracellular sites

SpyTag-Cell Perm. Peptide



D Multimeric-enzyme reactor assembly

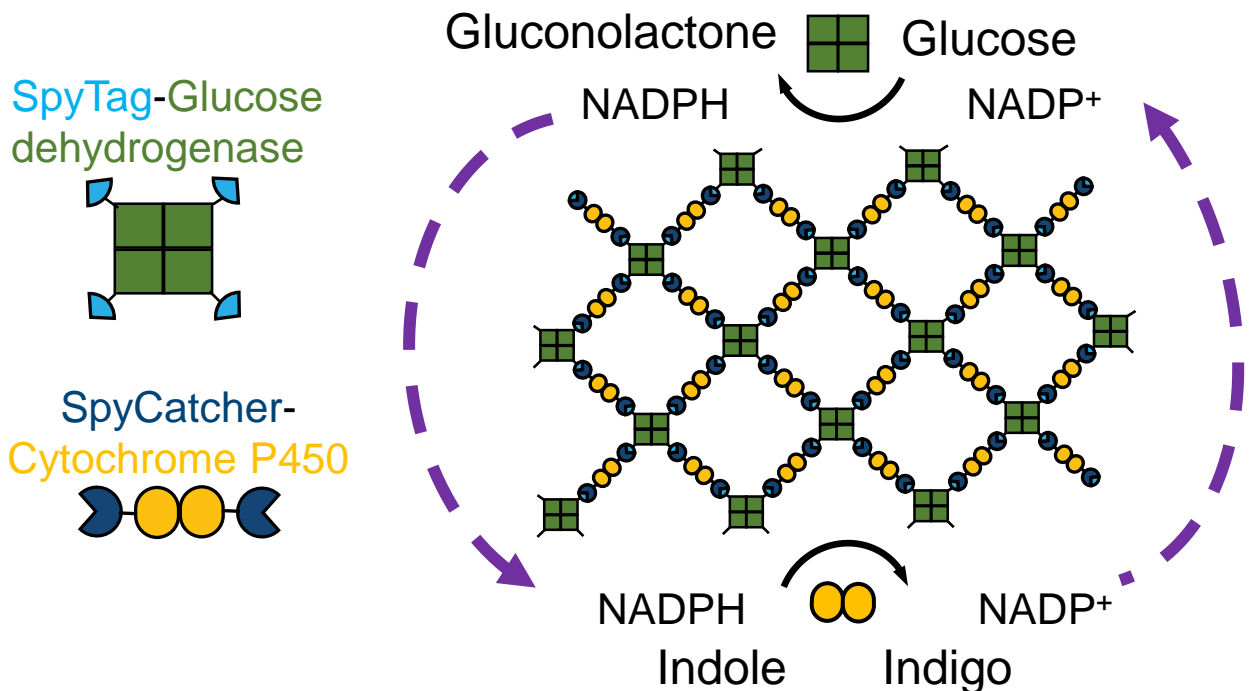


Table 1

Publication title	Journal name or Patent	Corresponding author	doi or patent code	Publication or priority date YEAR MONTH DAY)	Construct name (and Seq ID from patent)	Expression host	Compartment expressed (cytosol, periplasm, membrane, secreted, in vitro)	N-term, C-term, internal	AA sequence (Tag or Catcher bold red, linker where annotated in blue and underlined, * stop codon)
Plug-and-Display: decoration of Virus-Like Particles via isopeptide bonds for modular immunization.	Sci Rep.	Mark Howarth	10.1038/srep19234	2016 01 19	SpyCatcher-VLP (aka ΔN1-SpyCatcher-AP205CP3)	E. coli C41	cytosol	N-term SpyCatcher	MGSSHHHHHHGSG DSATHIKFS KRDEDEGKELAGATMELRDSSGK TISTWISDGQVKDFLYPGKYTFV ETAAPDGYEVATAITFTVNEQQG VTVNGKATKGDHIGSGSGSGS <u>G</u> ANKPMQPITSTANKIVWSDPTRL STTFASLLRQRVKVIAELNNVVS GQYVSVYKRPAPKPEGCADACVI MPNENQSIRTVISGSAENLATLKA EWETHKRNVDTLFASGNAGLGFL DPTAAIVSSDTTA*
Programmed loading and rapid purification of engineered bacterial microcompartment shells	Nat Commun	Cheryl A. Kerfeld	10.1038/s41467-018-05162-z	2018 07 23	pET11n::HTST	E. coli BL21 (DE3)	cytosol	Internal SpyTag	MDHAPERFDATPPAGEPDRPAL GVLELTSIARGITVADAALKRAP SLLLMSRPVSSGKHLLMMRGQ VAEVEESMIAAREIAGAG <u>GGGSG</u> <u>GS</u> <u>AHIVMVDAYKPTK</u> <u>GGSGGS</u> <u>G</u> ALLDELELPYAHEQLWRFLDA PVVADAWEDTESVIVETATVC AAIDSADAALKTAPVVLRDMRLA IGIAGKAFFTLTGELADVEAAAE VVRERCGARLLELACIARPVDEL RGRLFF*